THE JOURNAL OF PHYSICAL CHEMISTRY Letters

Letter

pubs.acs.org/JPCL

Low-Scaling Quantum Chemistry Approach to Excited-State Properties via an ab Initio Exciton Model: Application to Excitation Energy Transfer in a Self-Assembled Nanotube

Adrian F. Morrison and John M. Herbert*

Department of Chemistry and Biochemistry, The Ohio State University, Columbus, Ohio 43210, United States

ABSTRACT: We introduce a charge-embedding scheme for an excited-state quantum chemistry method aimed at weakly interacting molecular aggregates. The Hamiltonian matrix for the aggregate is constructed in a basis of direct products of configuration-state functions for the monomers, and diagonalization of this matrix affords excitation energies within ∼0.2 eV of the corresponding supersystem calculation. Both the basis states and the coupling matrix elements can be computed in a distributed way, resulting in an algorithm whose time-to-solution is independent of the number of chromophores, and we report calculations on systems with almost 55 000 basis functions using fewer than 450 processors. In a semiconducting organic nanotube, we find evidence of ultrafast, coherent dynamics followed by energy localization driven by static disorder. Truncation of the model system has a qualitative effect on the energy-transfer dynamics, demonstrating the importance of simulating an extended portion of the nanotube, which is not feasible using traditional quantum chemistry.

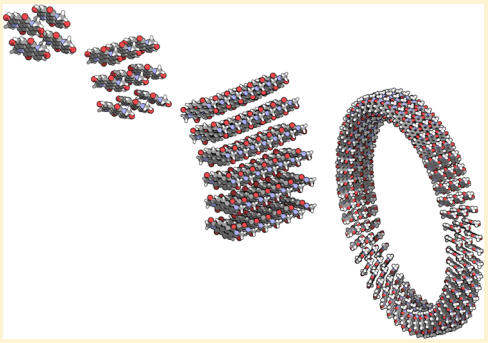

Excitation energy transfer is a fundamental step in both natural and artificial light-harvesting systems, and quantum chemical approaches can provide crucial mechanistic insight into these processes. A well-studied example is the Fenna−Matthews−Olson (FMO) complex, where the suggestion that quantum coherence enhances the energy-transfer rate has received significant attention.[1−3] The FMO complex is a trimer in which each monomer is composed of eight bacteriochlorophyll chromophores; hence, ab initio description of the chromophores within a single monomer is already fairly ambitious using traditional excited-state electronic structure methods, yet semiempirical studies have shown that consideration of the full trimer has a significant impact on the energy-transfer dynamics, even within a single monomer of the FMO trimer.[4] In simulations, the role of quantum coherence in FMO is highly sensitive to how the chromophore energies and couplings between them are described,[5,6] and recent model studies of the full light-harvesting complex (involving thousands of bacteriochlorophylls) have demonstrated efficient long-range energy transfer in these nanoscale systems.[7] Large-scale, atomistic ab initio studies may provide valuable insight into energy transfer in light-harvesting systems, organic photovoltaics, and other interesting optical materials, yet these calculations are prohibitively expensive using traditional ab initio quantum chemistry.

The challenge stems from the steep computational scaling of quantum chemistry with respect to system size combined with the sizable model systems necessary to describe solar light harvesting. The cost of even the most affordable ab initio methods for excited states grows as the fourth power of system size. Moreover, traditional quantum chemistry methods (at least when they are optimized for efficiency on one or a few processors) tend to scale poorly on modern, massively parallel platforms and are thus fundamentally ill-suited to scale to peta- or exa-scale computer architectures. Conversely, software that is highly scalable is often comparatively slow for small- or medium-size jobs run on a modest number of processors. To take highly efficient codes and scale them to large numbers of processors, new paradigms are needed.

Our approach to this challenge is based on the idea of a molecular exciton model.[8−10] Within such a model, collective excited states of an aggregate are represented as superpositions of excitations localized on molecular sites. The wave function for such a state can be expressed as

$$|\Xi_I\rangle = \sum_{n}^{\text{sites}} \sum_{i}^{\text{states}} K_n^{Ii} |\Psi_n^i\rangle \prod_{m\neq n} |\Psi_m\rangle \tag{1}$$

where $|\Psi_n^i\rangle$ represents an excited state of monomer n and $|\Psi_m\rangle$ is the ground-state wave function for monomer m. This ansatz is quite flexible; additional excited states i can be included to increase the variational flexibility of the basis,[10] and the basis can be further expanded to include charge-transfer excitons (in which an electron is transferred between monomers) or multiexciton states in which several molecular sites are excited simultaneously. The coefficients K_n^{Ii} are determined by diagonalizing the Hamiltonian in the exciton-site basis.

Received: September 22, 2015
Accepted: October 19, 2015

DOI: 10.1021/acs.jpclett.5b02109
J. Phys. Chem. Lett. 2015, 6, 4390−4396

Historically, matrix elements within the exciton framework are often approximated by taking the diagonal elements to be some estimates of the site energies and off-diagonal elements that are computed within a transition-dipole approximation. More recently, off-diagonal elements have been computed by numerical evaluation of the Coulomb integral between transition densities on different sites,[11−13] although this neglects exchange coupling. Our approach[10] is based on a fully ab initio realization of the ansatz in eq 1, in which basis states are constructed from independent configuration interaction-singles (CIS) calculations on individual monomers. The method is embarrassingly parallelizable because calculation of monomer basis states and coupling matrix elements can be distributed with near-unit parallel efficiency. As such, this model significantly outperforms parallel implementations of traditional single-excitation methods on equivalent hardware yet remains faithful to CIS excitation energies within ∼0.1 eV.[10]

Despite this favorable performance and parallel scalability, the cost to evaluate each individual matrix element scales as the fourth power of the overall size of the aggregate, as a result of the "corresponding orbitals" transformation[14] that is necessary to cope with the fact that orbitals on different monomers are not orthogonal.[10] In this work, we introduce a charge-embedding scheme that dramatically reduces the formal scaling and drastically increases performance while maintaining the accuracy and simplicity of the original approach. The efficiency of the new implementation enables us to treat system sizes well beyond the reach of traditional methods, with only modest hardware requirements.

Basis states in our model are constructed in the form of eq 1 from direct products of configuration state functions (CSFs) computed for each isolated monomer. The ground states of fragments *A*, *B*, *C*, ..., *F* are described by a single Hartree−Fock (HF) determinant, Φ_A. Excited states are described at the CIS level as linear combinations of singly-excited determinants Φ_A^{ia}:

$$|\Psi_A^*\rangle = \sum_{ia} C^{ia}|\Phi_A^{ia}\rangle \tag{2}$$

We use *i,j,k,...* and *a,b,c,...* to index occupied and virtual molecular spin−orbitals, respectively. To construct the exciton Hamiltonian, we need to evaluate matrix elements such as

$$\langle\Psi_A^*\Psi_B|\hat{H}|\Psi_A\Psi_B^*\rangle = \sum_{ia\sigma}\sum_{kb\tau} C_\sigma^{ia}C_\tau^{kb}\langle\Phi_A^{ia}\Phi_B|\hat{H}|\Phi_A\Phi_B^{kb}\rangle \tag{3}$$

Orbitals on different sites are not orthogonal; hence, Schrödinger's equation has the form of a generalized eigenvalue equation, and we must also compute overlap integrals such as

$$\langle\Psi_A^*\Psi_B|\Psi_A\Psi_B^*\rangle = \sum_{ia\sigma}\sum_{kb\tau} C_\sigma^{ia}C_\tau^{kb}\langle\Phi_A^{ia}\Phi_B|\Phi_A\Phi_B^{kb}\rangle \tag{4}$$

In these equations, we have introduced spin indices σ and τ in constructing CSFs from the monomer CIS calculations, as described in ref 10.

Matrix elements in eqs 3 and 4 are computed exactly, including full Coulomb and exchange coupling, using the generalized Slater−Condon rules[15] that can be derived following application of the corresponding orbital transformation.[14] To reduce the number of terms in eqs 3 and 4, we transform the individual monomer excited states into the basis of natural transition orbitals[16] (NTOs, which are equivalent to CIS natural orbitals[17]). Coefficients can then be discarded based on a controllable, occupation-number threshold, and this procedure generally results in no more than a few significant coefficients per monomer. For systems comprised of polar monomers, the accuracy can be improved if the individual monomer ground-state orbitals are computed using the "explicit polarization" (XPol) procedure,[18] a variational, self-consistent charge-embedding scheme. Our group has previously reported an implementation of XPol using "ChElPG" atomic charges derived from the electrostatic potential,[19,20] which are stable in large basis sets.

For brevity, the matrix elements in eqs 3 and 4 are given for the dimer *AB*, but in fact the basis states are direct products over all monomers, for example, $|\Psi_A^*\Psi_B\Psi_C\cdots\Psi_F\rangle$. Such a treatment is, in principle, required for *exact* Coulomb and exchange coupling. As a result of the corresponding orbitals transformation, the rate-limiting step in the calculation of any individual matrix element is the calculation of two-electron integrals for the entire system and their digestion with generalized density matrices for a particular monomer.[10] However, because the exchange interaction is short-ranged and the Coulomb interaction can be approximated via charge embedding, we propose here to retain the direct product ansatz but to simplify the evaluation of the matrix elements by partitioning the electronic coordinates in such a way as to distinguish significant and insignificant interfragment interactions:

$$\begin{aligned}&\langle\Psi_A^*\Psi_B\Psi_C\Psi_D|\hat{H}|\Psi_A\Psi_B^*\Psi_C\Psi_D\rangle\\ &\quad\approx \langle\Psi_A^*\Psi_B|\langle\Psi_C|\langle\Psi_D|\hat{H}_{AB} + \hat{V}_{\mathrm{QM}} + \hat{H}_C + \hat{H}_D\\ &\qquad + \hat{V}'_{\mathrm{MM}}|\Psi_A\Psi_B^*\rangle|\Psi_C\rangle|\Psi_D\rangle\end{aligned} \tag{5}$$

Such partition divides the system into two regions for which we adopt the terminology of "QM" and "MM". Coulomb and exchange interactions for all electrons in the significant (QM) region are treated exactly, and interfragment interactions with electrons in the less-signicant (MM) region are approximated as point charges. All *intra*-fragment interactions are described at the HF level.

Neglecting interfragment orbital overlap within the MM region, we can evaluate eq 5 as

$$\begin{aligned}&\langle\Psi_A^*\Psi_B\Psi_C\Psi_D|\hat{H}|\Psi_A\Psi_B^*\Psi_C\Psi_D\rangle\\ &\quad\approx \langle\Psi_A^*\Psi_B|\hat{H}_{AB} + \hat{V}_{\mathrm{QM}}|\Psi_A\Psi_B^*\rangle + (E_C + E_D + V'_{\mathrm{MM}})\langle\Psi_A^*\Psi_B|\Psi_A\Psi_B^*\rangle\end{aligned} \tag{6}$$

where E_C and E_D are the ground-state HF energies for the isolated fragments *C* and *D*. The operator

$$\hat{V}_{\mathrm{QM}} = \sum_{I\in\mathrm{MM}}\sum_{i\in\mathrm{QM}} \frac{q_I}{|\mathbf{R}_I - \mathbf{r}_i|} \tag{7}$$

describes the interaction between the QM and MM regions. Matrix elements of $\hat{V}_{\mathrm{QM}}$ are evaluated analogously to those for the core (one-electron) Hamiltonian; see eq 12 of ref 10. The quantity

$$\begin{aligned}V'_{\mathrm{MM}} = \frac{1}{2}\sum_{I\in\mathrm{MM}}{\sum_{J\in\mathrm{MM}}}' \frac{q_I q_J}{|\mathbf{R}_I - \mathbf{R}_J|} + \sum_{I\in\mathrm{QM}}\sum_{J\in\mathrm{MM}} \frac{Z_I q_J}{|\mathbf{R}_I - \mathbf{R}_J|}\\ + \sum_{I\in\mathrm{QM}}\sum_{J\in\mathrm{QM}} \frac{Z_I Z_J}{|\mathbf{R}_I - \mathbf{R}_J|}\end{aligned} \tag{8}$$

DOI: 10.1021/acs.jpclett.5b02109
J. Phys. Chem. Lett. 2015, 6, 4390−4396

describes the self-interaction of the point charges in the MM region, with the primed summation restricted to fragments $J \neq I$.

There is some flexibility in how the system is partitioned. It is natural to include in the QM region those monomers that are excited in either the bra or the ket, as we have done with monomers A and B in eqs 5 and 6, but other nearby monomers might need to be included in the QM region in order to capture exchange effects. We have implemented the charge-embedding scheme in a dynamic way so that fragments within a user-definable distance threshold from any excited fragments are automatically included in the QM region. We will investigate the accuracy of the method as a function of this threshold.

Results for the lowest singlet and triplet excited states of small water clusters are presented in Figure 1, and those for

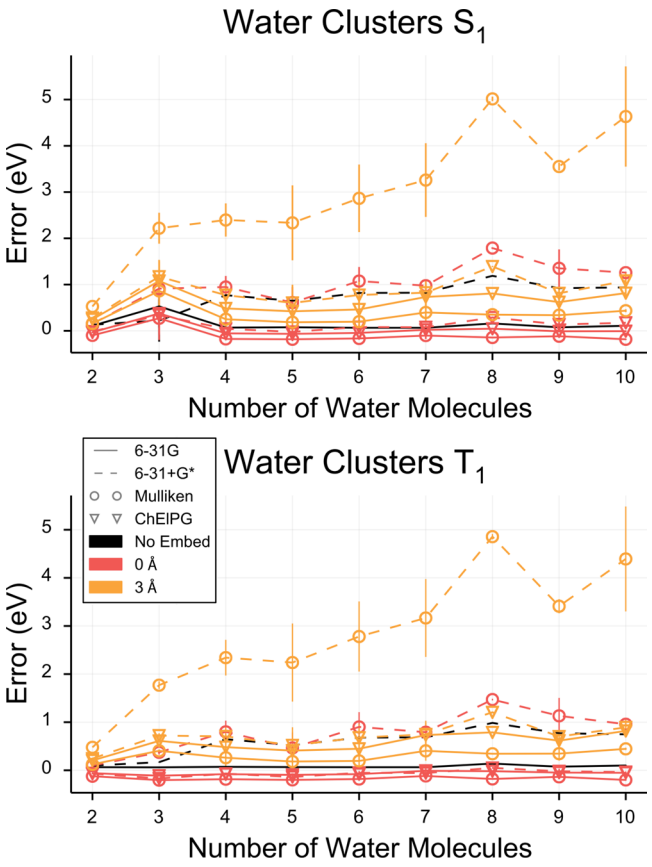

Figure 1. Mean unsigned errors in excitation energies, relative to supersystem CIS results, for various water cluster isomers. (Vertical lines represent the standard deviation.) Results without embedding correspond to the original ab initio exciton model of ref 10, and the "0 Å" threshold means that only the excited monomers are included in the QM region. All of the exciton calculations use XPol monomer wave functions and one CIS excited state per monomer. Cluster geometries are taken from ref 21.

several geometries of a $(H_2O)_{117}$ cluster are in Figure 2. Both sets of calculations use XPol self-consistent embedding for the monomer calculations, which adds minimal extra cost but was shown to be important in previous work, specifically in the case of water clusters where strong hydrogen-bonding interactions may significantly deform the H_2O molecular orbitals.[10] We examine the use of both Mulliken and ChElPG embedding charges. It is immediately clear from these results that the use of Mulliken charges in the 6-31+G* basis set leads to significantly

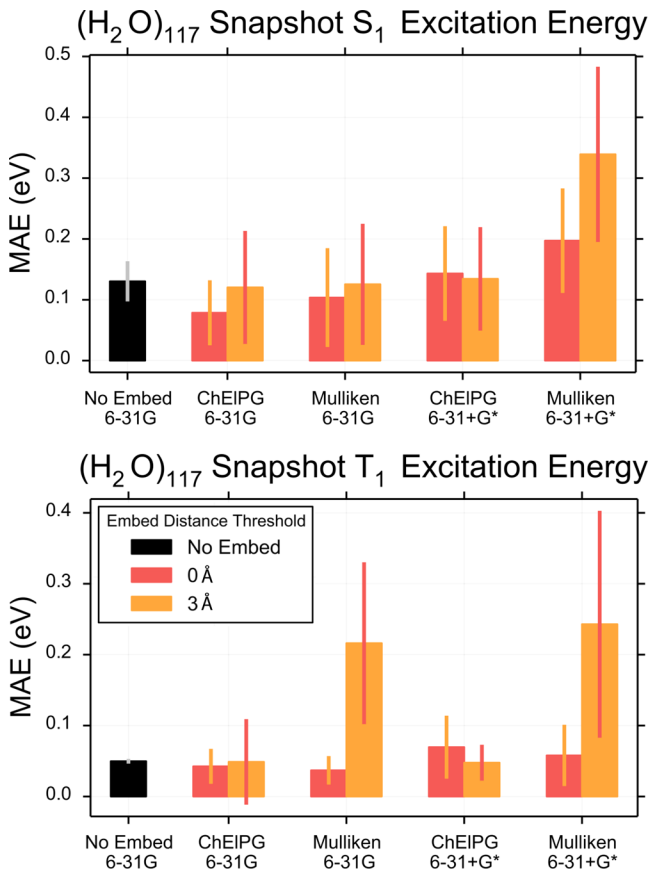

Figure 2. Mean absolute errors in excitation energies, relative to supersystem CIS results, for five snapshots extracted from a liquid water simulation. (Vertical lines represent the standard deviation.) Results without embedding correspond to the original ab initio exciton model of ref 10, and the "0 Å" threshold means that only the excited monomers are included in the QM region. All of the exciton calculations use XPol monomer wave functions and one CIS excited state per monomer.

larger errors as compared to other approaches, which is not surprising given the generally unreliable behavior of Mulliken charges in the presence of diffuse functions. Apart from this anticipated outlier, however, all of the errors are much smaller, and results using a "0 Å" embedding threshold (meaning that only those monomers that are excited in the bra or the ket are included in the QM region) generally lie within a few tenths of an eV from supersystem CIS excitation energies. Results for $(H_2O)_{117}$ (Figure 2) are even better, with errors $\lesssim 0.1$ eV when ChElPG embedding charges are used.

Results using a 3 Å embedding threshold are reasonably close to the 0 Å results and also close to results from the original model in which all of monomers are described at the QM level. Note that a nonzero distance threshold does introduce a degree of inconsistency, however, especially for water clusters, because the number of QM monomers varies from one calculation to the next. In matrix elements of the form $\langle \Psi_A^* \Psi_B \Psi_C \cdots | \hat{H} | \Psi_A \Psi_B^* \Psi_C \cdots \rangle$, the two excited monomers A and B may not be spatially proximal; thus, in the case of $(H_2O)_{117}$, a 3 Å cutoff around each of A and B results in anywhere from 20 H_2O molecules in the QM partition (when A and B are nearby) up to 50 QM H_2O molecules (when they are not). This added expense and inconsistency seems unjustified based on the accuracy of the 0 Å results. The latter calculations run up to 6

DOI: 10.1021/acs.jpclett.5b02109
J. Phys. Chem. Lett. 2015, 6, 4390−4396

times faster than full supersystem CIS calculations when both calculations are parallelized over a single, 20-core node using Q-Chem v. 4.3.1.[22] We will use the 0 Å threshold exclusively in what follows.

We next consider results for various organic chromophores, which are perhaps more realistic target systems for the exciton model. Systems examined here include tetracene, which has been widely studied in the context of singlet fission;[23−25] naphthalene diimide (NDI), which self-assembles into a nanotube with potentially interesting excited-state dynamics;[26,27] and guanine-cytosine (G-C) base pairs because exciton models have long been employed to understand DNA photophysics.[28−31] In the latter system, we find that a judicious definition of the fragments is paramount for accurate description of the delocalized states. Watson−Crick base pairs provide a better description of the T_1 state, while π-stacked G-C pairs along the same strand prove to be a better choice for the S_1 state. Results in Table 1 show that the charge-embedding

Table 1. Absolute Errors[a] (in eV) in Excitation Energies for Organic Chromophores Using the ab Initio Exciton Model[b]

		6-31G		6-31+G*	
	F	none	ChElPG	none	ChElPG
			$(NDI)_F$		
T_1	2	0.14	0.14	0.14	0.13
	4	0.14	0.15	0.14	0.13
S_1	2	0.12	0.12	0.12	0.12
	4	0.17	0.17	0.16	0.11
			$(tetracene)_F$		
T_1	2	0.16	0.16	0.16	0.16
	4	0.15	0.15	0.15	0.16
S_1	2	0.15	0.10	0.15	0.16
	4	0.19	0.18	0.19	0.20
			$(guanine\text{-}cytosine)_F$[c]		
T_1[d]	2	0.18	0.14	0.07	0.09
	4	0.13	0.18	0.08	0.13
S_1[e]	2	0.11	0.00	0.03	0.10
	4	0.18	0.08	0.24	0.07

[a]Relative to supersystem CIS with the same basis set. [b]Using an 85% NTO threshold. [c]Using XPol monomer wave functions. [d]Watson−Crick base pairs used as exciton sites. [e]π-Stacked base pairs used as exciton sites.

scheme performs quite well, with errors relative to supersystem calculations of 0.1−0.2 eV for all systems. This level of error is consistent with that obtained in our previous version of the model, in which all monomers were described at a QM level.

Regarding computational performance, even without charge embedding, the ab initio exciton model exhibits better parallel scalability and outperforms traditional CIS calculations.[10] This is despite the fact that the cost of calculating each matrix element scales as $O(N^x)$ with respect to the size of the entire supersystem, N, where the exponent x reflects the cost of computing electron repulsion integrals. (The oft-quoted value[32] $x = 4$ is correct for small molecules, but trivial integral screening will reduce this to $x = 2$ even for medium-size systems.) Charge embedding reduces the scaling of exciton calculations to $O(F^2 \times n_{\text{pair}}^x)$, where n_{pair} represents the size of a pair of monomers. Parallel efficiency remains excellent as the matrix elements can be computed entirely independently of one another and are thus distributable without communication or cache coherency overhead. We have implemented the method in Q-Chem using distributed-memory MPI parallelization that allows scaling across multiple nodes, and with enough cores, the time-to-solution can be made to scale as $O(n_{\text{pair}}^x)$ regardless of the size of the supersystem.

In Figure 3, we compare the parallel scaling performance to that of a multithreaded implementation of CIS for G-C base

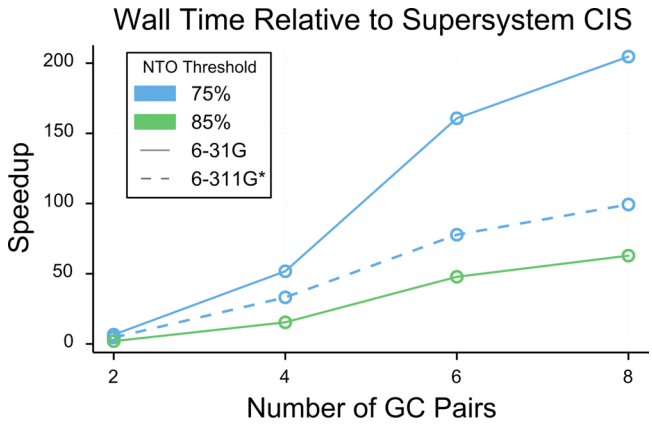

Figure 3. Parallel performance of the exciton model relative to a multithreaded (OpenMP) version of supersystem CIS, as implemented in Q-Chem v. 4.3.1. Calculations were run on $F(F-1)/2$ cores up to $F = 20$, which is the number of cores on a node.

stacks. (The speedup is defined as the ratio of the wall time required for a supersystem CIS calculation to that required for the exciton calculation when both calculations are run on the same number of processors.) In previous work,[10] we compared parallel efficiency versus NWChem[33] due to the good scalability of that code. However, Q-Chem's multithreaded CIS code is much faster than NWChem's on a small numbers of processors; therefore, the performance of the exciton model is evaluated here versus Q-Chem. The comparison is limited to a single node (20 processors) because Q-Chem's CIS implementation does not scale well across multiple nodes. This means that even greater speedups are possible for the largest systems in Figure 3 because the exciton model does not suffer any performance degradation when extended beyond a single node. Nevertheless, we still observe speedups of up to 200× using an NTO threshold of 75% that was sufficient to achieve ∼0.2 eV accuracy in previous calculations.[10] Note that the both NTO threshold and the size of the atomic orbital basis set contribute only prefactors to the $O(F^2 \times n_{\text{pair}}^x)$ scaling, independent of the overall size of the system.

This scalability allows us to treat systems that would otherwise be intractable on commodity hardware and would instead require running a code like NWChem on thousands of processors (or more). As a demonstration, we have performed calculations on $(NDI)_F$ substructures of varying sizes taken from the nanotube structural model in ref 27. Table 2 shows

Table 2. Resources Required for an Exciton Calculation[a] on Different $(NDI)_F$ Nanotube Substructures

F =	2	4	9	42	156
no. basis functions	876	1752	3942	14 700	54 600
no. processors	3	10	20	150	440

[a]In less than 1 week of wall time.

DOI: 10.1021/acs.jpclett.5b02109
J. Phys. Chem. Lett. 2015, 6, 4390−4396

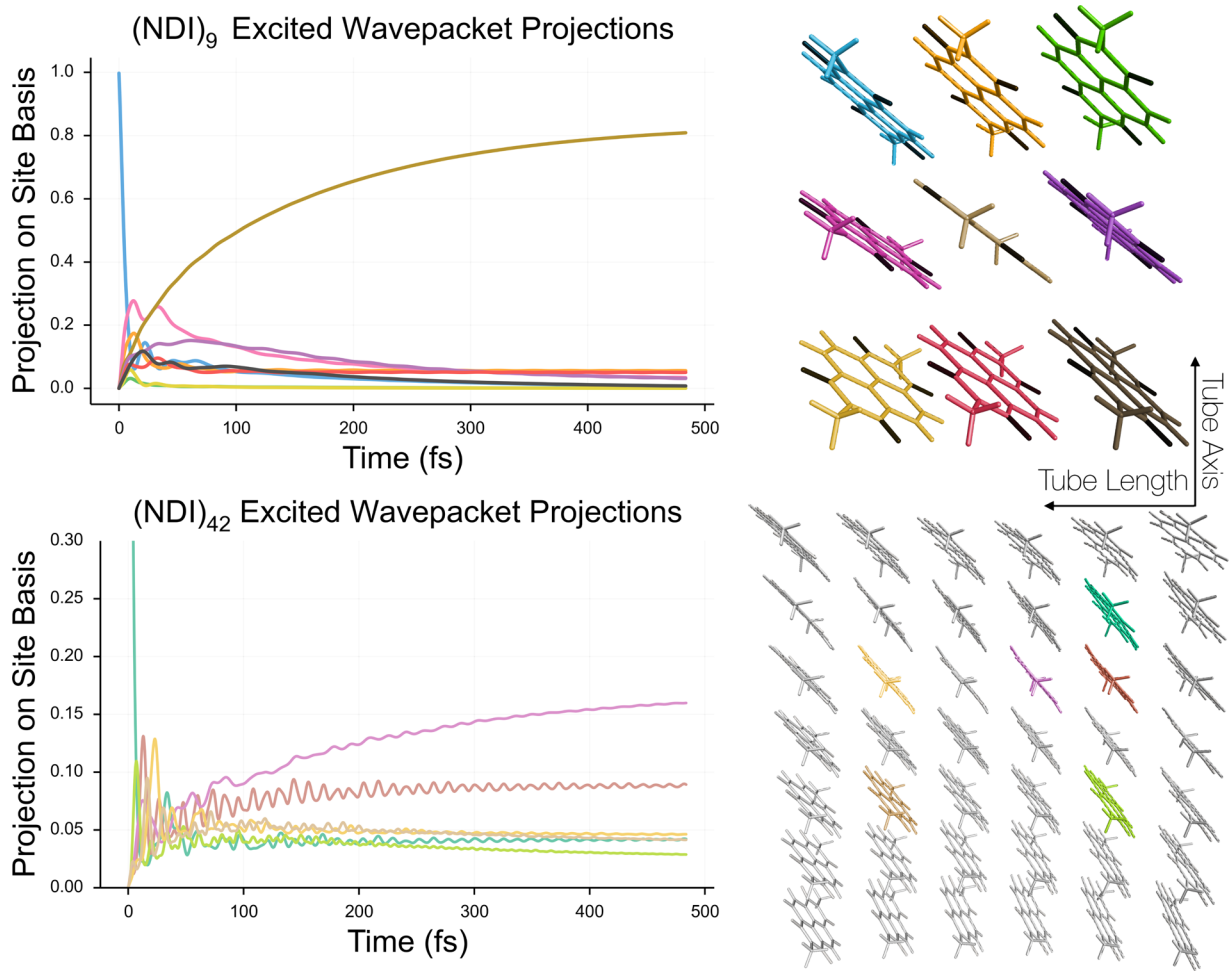

Figure 4. Redfield dynamics of 9- and 42-monomer substructures of an organic semiconductor nanotube. The initial wavepacket is localized on a single exciton-site basis state, and the plots on the left show the projections of the wavepacket onto various other basis states, which are color-coded according to the figures on the right.

the size of each system (in terms of the number of basis functions) and the number of processors on which it was run; in each case, the calculation was complete in under 1 week. As shown in the table, our method can be applied to nanoscale systems with upward of 50 000 basis functions on hardware that might readily be available in a laboratory cluster.

A uniquely valuable aspect of an exciton model is the unambiguous diabatic representation of localized excited states that is inherent in the exciton-site basis. Using operators in this basis, it is very straightforward to use a density matrix formalism to study excitation energy transfer in extended systems, and we have used the Redfield master equation[34−37] to investigate exciton dynamics in substructures of the NDI nanotube. In this approach, system−bath interactions are entirely described by a spectral density function $S(\omega)$, for which we use a temperature bath spectral density with an Ohmic form and a Lorentzian cutoff:

$$S(\omega) = \left(\frac{2\omega\lambda\Omega}{\omega^2 + \Omega^2}\right) n_{\mathrm{BE}}(\omega) \tag{9}$$

The parameters λ and Ω are the reorganization energy and the characteristic bath cutoff frequency, respectively, and $n_{\mathrm{BE}}(\omega)$ is the Bose−Einstein distribution. The parameters were computed from excited-state geometry optimization and frequency calculations on a NDI monomer at the same level of theory that is used in the exciton calculations, CIS/6-31G* . (The values are λ = 0.013 au and $\hbar\Omega$ = 0.015 au.) Although the spectral density in eq 9 can sometimes average out potentially important details of the vibrational structure[38] and Redfield theory itself has known shortcomings,[39] in the regime of weak electron−nuclear coupling, this approach is a simple and computationally tractable way to probe ultrafast electronic processes and has provided insight in various contexts.[40−42]

Quantum dynamics calculations were performed on $(NDI)_9$ and $(NDI)_{42}$, starting from an initial wavepacket corresponding to populating an excited state on a single NDI monomer. The density matrix was propagated in time (using the QuTiP software[43]), and projections onto the significant exciton-site basis states are plotted in Figure 4. Following a period of <50 fs in which the initial state delocalizes over multiple monomers, the dynamics in both NDI substructures are dominated by a 100−500 fs time period during which the excitation relocalizes on a different monomer. This is primarily the result of static disorder; excitation energy flows downhill to a monomer that is lower in energy. (Heterogeneity in the site energies is easily confirmed by examining the diagonal elements of the exciton Hamiltonian.) These observations are generally in agreement with results presented in ref 27, where an incoherent hopping model based on pairwise couplings and Fermi's Golden Rule predicts energy-transfer time scales ranging from 0.2 to 1.0 ps.

DOI: 10.1021/acs.jpclett.5b02109
J. Phys. Chem. Lett. 2015, 6, 4390−4396

One point that is specifically raised in ref 27 is the importance of atomistic resolution in the electronic structure studies because even small variations in the site energies of an otherwise homogeneous system are enough to significantly modulate the flow of energy.

We selected $(NDI)_9$ for this comparison because it was the model system used in time-dependent density functional theory (TDDFT) calculations in ref 27, where the primary limitation to the system size is a serious memory bottleneck due to the large density of states. Those calculations were performed at the TDDFT/3-21G* level, and to locate the lowest-energy bright state of $(NDI)_9$ at the TDDFT/6-31+G* level, we estimate that ∼30 Gb would be required to store the subspace vectors for the Davidson iterations. No such bottleneck exists in the exciton model.

In view of this, another crucial message from these calculations is the significant, qualitative difference between the exciton dynamics in $(NDI)_9$ versus $(NDI)_{42}$. The former exhibits rapid dephasing, with coherent oscillations in the site populations only within the first 100 fs, whereas in the larger model, the population transfer is coherent for nearly 500 fs. This is understandable as the greater number and range of couplings in the larger system provides more instances of accidental degeneracies in the site energies, whereas the nine-unit model is much more susceptible to "edge effects" in the distribution of energies and couplings. The distinct differences between these two simulations highlights the benefit of large-scale simulations as coherence can significantly alter the energy-transfer time scale. The results suggest that this nanotube, and similar systems, undergoes ultrafast coherent excitation energy transfer that can potentially be guided through strategic functionalization of the monomers. Our ab initio exciton model, in its more efficient formulation presented here, is well suited to investigate such processes.

In summary, we have significantly improved the performance of our ab initio exciton model without sacrificing its accuracy or physically-motivated simplicity. Tests on water clusters as large as $(H_2O)_{117}$ indicate that only a minimum number of monomers need be treated quantum-mechanically in computing matrix elements of the exciton Hamiltonian, eliminating a key bottleneck in our original implementation of the method. Accuracy of ∼0.1−0.2 eV with respect to supersystem CIS calculations is obtained for these systems as well as for coupled organic chromophores such as tetracene and DNA nucleobases. The embarrassingly-parallelizable nature of the method, combined with the fact that the cost of each matrix element does not increase with (super)system size in our new formulation, allows us to treat systems that would be completely intractable with conventional approaches, using only commodity hardware. Preliminary studies of excitation energy transfer in substructures of an organic semiconductor nanotube demonstrate that large-scale simulations may suggest qualitatively different energy flow as compared to the smaller models that are the only tractable choices when applying conventional approaches.

Further extensions of the model are possible and become more feasible due to the reduced cost of the implementation reported here. Inclusion of electron correlation effects in the monomer excited-state calculations will be crucial for obtaining accurate values for the on-site energies, for example, but should be feasible within a perturbative framework.[44,45] Because the model comes with a well-defined wave function for the collective excitation, molecular properties (such as transition moments) are straightforward to calculate. Such developments are currently underway in our group.

AUTHOR INFORMATION

Corresponding Author

*E-mail: herbert@chemistry.ohio-state.edu.

Notes

The authors declare no competing financial interest.

ACKNOWLEDGMENTS

This work was supported by the U.S. Department of Energy, Office of Basic Energy Sciences, Division of Chemical Sciences, Geosciences, and Biosciences under Award No. DE-SC0008550. Calculations were performed at the Ohio Supercomputer Center under project PAA-0003.[46] J.M.H. is a Camille Dreyfus Teacher−Scholar.

REFERENCES

(1) Engel, G. S.; Calhoun, T. R.; Read, E. L.; Ahn, T.-K.; Mancala, T.; Cheng, Y.-C.; Blankenship, R. E.; Fleming, G. R. Evidence for Wavelike Energy Transfer through Quantum Coherence in Photosynthetic Systems. *Nature* **2007**, *446*, 782−786.

(2) Scholes, G. D.; Fleming, G. R.; Olaya-Castro, A.; van Grondelle, R. Lessons from Nature about Solar Light Harvesting. *Nat. Chem.* **2011**, *3*, 763−774.

(3) Chenu, A.; Scholes, G. D. Coherence in Energy Transfer and Photosynthesis. *Annu. Rev. Phys. Chem.* **2015**, *66*, 69−96.

(4) Olbrich, C.; Jansen, T. L. C.; Liebers, J.; Aghtar, M.; Strümpfer, J.; Schulten, K.; Knoester, J.; Kleinekathöfer, U. From Atomistic Modeling to Excitation Transfer and Two-Dimensional Spectra of the FMO Light-Harvesting Complex. *J. Phys. Chem. B* **2011**, *115*, 8609−8621.

(5) Jurinovich, S.; Curutchet, C.; Mennucci, B. The Fenna-Matthews-Olson Protein Revisited: A Fully Polarizable (TD)DFT/MM Description. *ChemPhysChem* **2014**, *15*, 3194−3204.

(6) Shim, S.; Rebentrost, P.; Valleau, S.; Aspuru-Guzik, A. Atomistic Study of the Long-Lived Quantum Coherences in the Fenna-Matthews-Olson Complex. *Biophys. J.* **2012**, *102*, 649−660.

(7) Huh, J.; Saikin, S. K.; Brookes, J. C.; Valleau, S.; Fujita, T.; Aspuru-Guzik, A. Atomistic Study of Energy Funneling in the Light-Harvesting Complex of Green Sulfur Bacteria. *J. Am. Chem. Soc.* **2014**, *136*, 2048−2057.

(8) Frenkel, J. On the Transformation of Light into Heat in Solids. I. *Phys. Rev.* **1931**, *37*, 17−44.

(9) Davydov, A. S. The Theory of Molecular Excitons. *Soviet Physics Uspekhi* **1964**, *7*, 145−178.

(10) Morrison, A. F.; You, Z.-Q.; Herbert, J. M. Ab Initio Implementation of the Frenkel-Davydov Exciton Model: A Naturally Parallelizable Approach to Computing Collective Excitations in Crystals and Aggregates. *J. Chem. Theory Comput.* **2014**, *10*, 5366−5376.

(11) Krueger, B. P.; Scholes, G. D.; Fleming, G. R. Calculation of Couplings and Energy-Transfer Pathways between the Pigments of LH2 by the ab Initio Transition Density Cube Method. *J. Phys. Chem. B* **1998**, *102*, 5378−5386.

(12) Tretiak, S.; Zhang, W. M.; Chernyak, V.; Mukamel, S. Excitonic Couplings and Electronic Coherence in Bridged Naphthalene Dimers. *Proc. Natl. Acad. Sci. U. S. A.* **1999**, *96*, 13003−13008.

(13) Czader, A.; Bittner, E. R. Calculations of the Exciton Coupling Elements between the DNA Bases using the Transition Density Cube Method. *J. Chem. Phys.* **2008**, *128*, 035101/1−035101/12.

(14) Amos, A. T.; Hall, G. G. Single Determinant Wave Functions. *Proc. R. Soc. London, Ser. A* **1961**, *263*, 483−493.

(15) King, H. F.; Stanton, R. E.; Kim, H.; Wyatt, R. E.; Parr, R. G. Corresponding Orbitals and the Nonorthogonality Problem in Molecular Quantum Mechanics. *J. Chem. Phys.* **1967**, *47*, 1936−1941.

DOI: 10.1021/acs.jpclett.5b02109
J. Phys. Chem. Lett. 2015, 6, 4390−4396

(16) Martin, R. L. Natural Transition Orbitals. *J. Chem. Phys.* **2003**, *118*, 4775−4777.
(17) Surján, P. R. Natural Orbitals in CIS and Singular-Value Decomposition. *Chem. Phys. Lett.* **2007**, *439*, 393−394.
(18) Xie, W.; Song, L.; Truhlar, D. G.; Gao, J. The Variational Explicit Polarization Potential and Analytical First Derivative of Energy: Towards a Next Generation Force Field. *J. Chem. Phys.* **2008**, *128*, 234108:1−9.
(19) Herbert, J. M.; Jacobson, L. D.; Un Lao, K.; Rohrdanz, M. A. Rapid Computation of Intermolecular Interactions in Molecular and Ionic Clusters: Self-Consistent Polarization Plus Symmetry-Adapted Perturbation Theory. *Phys. Chem. Chem. Phys.* **2012**, *14*, 7679−7699.
(20) Holden, Z. C.; Richard, R. M.; Herbert, J. M. Periodic Boundary Conditions for QM/MM Calculations: Ewald Summation for Extended Gaussian Basis Sets. *J. Chem. Phys.* **2013**, *139*, 244108/1−244108/13.
(21) Temelso, B.; Archer, K. A.; Shields, G. C. Benchmark Structures and Binding Energies of Small Water Clusters with Anharmonicity Corrections. *J. Phys. Chem. A* **2011**, *115*, 12034−1204.
(22) Shao, Y.; Gan, Z.; Epifanovsky, E.; Gilbert, A. T. B.; Wormit, M.; Kussmann, J.; Lange, A. W.; Behn, A.; Deng, J.; Feng, X.; et al. Advances in Molecular Quantum Chemistry Contained in the Q-Chem 4 Program Package. *Mol. Phys.* **2015**, *113*, 184−215.
(23) Smith, M. B.; Michl, J. Singlet Fission. *Chem. Rev.* **2010**, *110*, 6891−6936.
(24) Zimmerman, P. M.; Musgrave, C. B.; Head-Gordon, M. A Correlated Electron View of Singlet Fission. *Acc. Chem. Res.* **2013**, *46*, 1339−1347.
(25) Casanova, D. Electronic Structure Study of Singlet Fission in Tetracene Derivatives. *J. Chem. Theory Comput.* **2014**, *10*, 324−334.
(26) Shao, H.; Seifert, J.; Romano, N. C.; Gao, M.; Helmus, J. J.; Jaroniec, C. P.; Modarelli, D. A.; Parquette, J. R. Amphiphilic Self-Assembly of an n-Type Nanotube. *Angew. Chem., Int. Ed.* **2010**, *49*, 7688−7691.
(27) Gao, M.; Paul, S.; Schwieters, C. D.; You, Z.-Q.; Shao, H.; Herbert, J. M.; Parquette, J. R.; Jaroniec, C. P. An Atomic Resolution Structural Model for a Self-Assembled Nanotube Provides Insight into its Exciton Dynamics. *J. Phys. Chem. C* **2015**, *119*, 13948−13956.
(28) Bouvier, B.; Gustavsson, T.; Markovitsi, D.; Millié, P. Dipolar Coupling between Electronic Transitions of the DNA Bases and its Relevance to Exciton States in Double Helices. *Chem. Phys.* **2002**, *275*, 75−92.
(29) Bouvier, B.; Dognon, J.-P.; Lavery, R.; Markovitsi, D.; Millié, P.; Onidas, D.; Zakrzewska, K. Influence of Conformational Dynamics on the Exciton States of DNA Oligomers. *J. Phys. Chem. B* **2003**, *107*, 13512−13522.
(30) Bittner, E. R. Lattice Theory of Ultrafast Excitonic and Charge-Transfer Dynamics in DNA. *J. Chem. Phys.* **2006**, *125*, 094909/1−094909/12.
(31) Bittner, E. R. Frenkel Exciton Model of Ultrafast Excited State Dynamics in AT DNA Double Helices. *J. Photochem. Photobiol., A* **2007**, *190*, 328−334.
(32) Schlegel, H. B.; Frisch, M. J. Computational Bottlenecks in Molecular Orbital Calculations. *Theoretical and Computational Models for Organic Chemistry*; Formosinho, S. G., Csizmadia, I. G., Arnaut, L. G., Eds.; Kluwer: Norwell, MA, 1991; pp 5−33.
(33) Valiev, M.; Bylaska, E. J.; Govind, N.; Kowalski, K.; Straatsma, T. P.; van Dam, H. J. J.; Wang, D.; Nieplocha, J.; Apra, E.; Windus, T. L.; et al. NWChem: A Comprehensive and Scalable Open-Source Solution for Large Scale Molecular Simulations. *Comput. Phys. Commun.* **2010**, *181*, 1477−1489.
(34) Redfield, A. G. The Theory of Relaxation Processes. In *Advances in Magnetic Resonance*; Advances in Magnetic and Optical Resonance, Vol. *1*; Waugh, J. S., Ed.; Academic Press: New York, 1965; pp 1−32.
(35) Breuer, H.-P.; Petruccione, F. *The Theory of Open Quantum Systems*; Oxford University Press: New York, 2002.
(36) Schröter, M. *Dissipative Exciton Dynamics in Light Harvesting Complexes*; Springer Spektrum: Heidelberg, Germany, 2015.
(37) Valkunas, L.; Abramavicius, D.; Mančal, T. *Molecular Excitation Dynamics and Relaxation*; Wiley-VCH Verlag GmbH and Co. KGaA;: Weinheim, Germany, 2013.
(38) Olbrich, C.; Strümpfer, J.; Schulten, K.; Kleinekathöfer, U. Theory and Simulation of the Environmental Effects on FMO Electronic Transitions. *J. Phys. Chem. Lett.* **2011**, *2*, 1771−1776.
(39) Ishizaki, A.; Fleming, G. R. On the Adequacy of the Redfield Equation and Related Approaches to the Study of Quantum Dynamics in Electronic Energy Transfer. *J. Chem. Phys.* **2009**, *130*, 234110/1−234110/8.
(40) Kühl, A.; Domcke, W. Effect of a Dissipative Environment on the Dynamics at a Conical Intersection. *Chem. Phys.* **2000**, *259*, 227−236.
(41) Chan, W.-L.; Berkelbach, T. C.; Provorse, M. R.; Monahan, N. R.; Tritsch, J. R.; Hybertsen, M. S.; Reichman, D. R.; Gao, J.; Zhu, X.-Y. The Quantum Coherent Mechanism for Singlet Fission: Experiment and Theory. *Acc. Chem. Res.* **2013**, *46*, 1321−1329.
(42) Rebentrost, P.; Mohseni, M.; Aspuru-Guzik, A. Role of Quantum Coherence and Environmental Fluctuations in Chromophoric Energy Transport. *J. Phys. Chem. B* **2009**, *113*, 9942−9947.
(43) Johansson, J. R.; Nation, P. D.; Nori, F. QuTiP 2: A Python Framework for the Dynamics of Open Quantum Systems. *Comput. Phys. Commun.* **2013**, *184*, 1234−1240.
(44) Head-Gordon, M.; Rico, R. J.; Oumi, M.; Lee, T. J. A Doubles Correction to Electronic Excited States from Configuration Interaction in the Space of Single Substitutions. *Chem. Phys. Lett.* **1994**, *219*, 21−29.
(45) Yost, S. R.; Kowalczyk, T.; Van Voorhis, T. A Multireference Perturbation Method using Non-Orthogonal Hartree-Fock Determinants for Ground and Excited States. *J. Chem. Phys.* **2013**, *139*, 174104/1−174104/9.
(46) *Ohio Supercomputer Center*. http://osc.edu/ark:/19495/f5s1ph73 (Accessed October 14, 2015).

DOI: 10.1021/acs.jpclett.5b02109
J. Phys. Chem. Lett. 2015, 6, 4390−4396